Histol Histopathol (2004) 19: 1125-1132

http://www.hh.um.es

Histology and Histopathology

Cellular and Molecular Biology

Cytoskeleton disruption in chondrocytes from a rat osteoarthrosic (OA) -induced model: its potential role in OA pathogenesis

N. Capín-Gutiérrez[1], P. Talamás-Rohana[1], A. González-Robles[1], C. Lavalle-Montalvo[3] and J.B. Kourí[1,2]

[1]Departamento de Patología Experimental y [2]Unidad de Microscopía Electrónica, Centro de Investigación y de Estudios Avanzados del Instituto Politécnico Nacional (CINVESTAV-IPN), México D.F. México and [3]Hospital General Xoco, México D.F., México

Summary. Morphological and functional changes of chondrocytes are typical in OA cartilage. In this work, we have described noteworthy changes in intermediate filaments cytoskeleton evidenced by transmission electron microscopy. Alterations in the distribution as well as in the content of vimentin, actin, and tubulin have been described by specific fluorescence labelling of each cytoskeletal component and confocal analysis. Normal vs OA cartilages showed a reduction in the percentage of labelled chondrocytes of 37.1% for vimentin, 4.7% for actin, and 20.1% for tubulin. Statistical analysis of fluorescence intensities (mean % ± SEM) between normal and OA rat cartilage revealed a highly significant difference in vimentin, a significant difference in tubulin, and a non-significant difference in actin. Moreover, by western blot, altered electrophoretic patterns were observed mainly for vimentin and tubulin in OA cartilage in comparison with normal cartilage. These results allow us to suggest that substantial changes in vimentin and tubulin cytoskeleton of chondrocytes might be involved in OA pathogenesis.

Key words: Osteoarthrosis, Cytoskeleton, Vimentin, Actin, Tubulin

Introduction

Osteoarthrosis (OA) is an chronic articular disease characterized by focal degeneration of the articular cartilage, and is associated with altered subchondral bone remodeling, bone hypertrophy, and the presence of osteophytes (Mankin et al., 1994). Chondrocytes within this scenario suffer dramatical changes in their morphology and physiology patterns as part of the pathogenesis of this disease (Mow et al., 1992).

Cytoskeleton, which establishes a close relationship with the extracellular matrix, plays an important role in cell shape and function. Studies on the structure and organization of actin, vimentin, and tubulin in normal chondrocytes have been reported (Zanetti et al., 1984; Hirsch et al., 1993; Benjamin et al., 1994; Idowu et al., 2000; Langelier et al., 2000). Changes in the organization of these proteins are linked to several pathological states (Pena et al., 1983; Takeda et al., 1992; Mashima et al., 1999; Bajo et al., 2001). This could also be the case for OA. However, the cytoskeleton in OA chondrocytes has been hardly studied. Our group made the first report about cytoskeleton disorder in chondrocytes from human OA. Using ultrastructural and immunohistochemistry procedures, we showed that upper-zone clustered chondrocytes from OA patients displayed a distorted distribution of actin, vimentin, and tubulin (Kouri et al., 1998). In the present work, using an experimentally induced OA model in rats, we studied whether cytoskeleton alterations were present during OA development. The use of an experimental model allowed us to perform the study without interference by variability factors present during human OA, such as the use of different drugs that condition the development of the cytoskeleton modifications (Egerbacher et al., 2000). Our results provided direct evidence that the cytoskeleton of OA-induced rat chondrocytes displayed remarkable modifications, similar to those reported in human OA chondrocytes (Kouri et al., 1998); therefore, we hypothesize that this disruption might play an important role in the OA pathogenesis.

Materials and methods

Tissue sampling

One hundred and eighty male Wistar rats (approximately 150 grams in weight each one) were included in this study. One hundred and twenty animals

Offprint requests to: Juan B. Kourí Flores, Centro de Investigación y de Estudios Avanzados (CINVESTAV-IPN) Ave. Instituto Politécnico Nacional No. 2508 Col. Sn. Pedro Zacatenco, Apartado Postal 14740, C.P. 07360 México D.F., México. Fax (5255) 5061-9890. e-mail: bkouri@mail.cinvestav.mx

were induced to OA by partial menisectomy as described previously (Abbud and Kouri, 2000), and 60 animals were used as non-surgery controls. All animals were trained for 20 min per day for 20 days after surgery to increase mechanical stress in the knees of both normal and OA-induced rats. Samples (cartilages together with a small portion of the subchondral bone) were removed from the weight-bearing areas of normal and fibrillated osteoarthrotic knee condyles (Kouri et al., 1996). The experimental procedures used followed the National Research Guidelines for laboratory animals in Mexico.

Transmission electron microscopy.

Cartilage samples from 15 normal and 30 OA-induced rats were cut into small fragments (2-3 mm), fixed in 2% glutaraldehyde-cacodylate buffer (0.15 M, pH 7.2) for 2 h at room temperature (RT), and post-fixed in 1% osmium tetroxide (OsO_4) in the same buffer for 2 h. Then they were dehydrated in gradually increasing concentrations of ethanol. Resin infiltration was done with a mixture of Spur resin/ethanol (1:3, 2:2, 3:1), and finally samples were embedded in pure Spur resin and polymerized at 60 °C for 24 h (Kouri et al., 2000).

Semi-thin sections of approximately 1 mm thickness were obtained from normal and OA samples with an ultramicrotome (Ultracut-E, Reichert Jung), stained with toluidine-blue and then treated with absolute ethanol to fade out over-stained sections. OA samples that displayed the most typical OA-induced changes were selected under a light microscope (Carl Zeiss III RS). Most damaged regions from 6 of these OA cartilages and 3 normal cartilages were thin-sectioned for ultrastructural observations. No less than 3 sections from each condition were studied. Samples were mounted on formvar-coated one-hole grids, and stained with uranyl acetate (30 min) and lead citrate (5 min), and were examined under JOEL JEM-2000 EX (Tokyo, Japan) and Philips Morgagni 268D (Holland) electron microscopes.

Immunohistochemistry

The entire zone of the articular cartilage and a small portion of the subchondral bone from 15 normal and 30 OA rats were cut. Slicing was not needed since this tissue is very thin in rats (approximately 1-1.5 mm). These fragments were fixed with 4% paraformaldehyde in PBS, pH 7.4, at 4 °C, from 4 to 8 h. Afterwards, they were incubated overnight in 10% sucrose at 4 °C. Samples were included in Tissutec (Tissue Freezing Medio-Hung), and perpendicularly cryosectioned (Leica Cryostat CM 1100; Heerbrugg, Switzerland) into 5-µm thick slices and mounted on gelatine-coated slides (gelatine 0.5%, chromium and potassium sulphate 0.05%). All samples were stained with toluidine blue to determine if they showed typical OA-induced changes. Ten normal and 10 OA cartilages were selected and stored for at least 2 days at -20 °C before further processing. These samples were hydrated in PBS and post-fixed for 5 min in acetone at -20 °C (Sigal et al., 1985; Kouri et al., 2002). Samples were blocked with 0.2% IgG-free bovine serum albumin (Sigma Chemical Co. St. Louis, Mo) in PBS-T (PBS containing 0.2% Triton X-100) for 20 min at RT, and incubated overnight at 4 °C in a wet chamber with the appropriate primary antibody: anti-vimentin 1:40 or anti-tubulin 1:20 (Biotechnology, Santa Cruz). After several washes, samples were incubated with FITC-conjugated goat anti-mouse IgG (1:60) (Vector Laboratories, Burlingame CA) for 1 h at RT. Primary antibodies were tested on HEp-2 cells (INOVA Diagnostic, Inc. San Diego). As negative controls, samples were incubated without the primary antibody and with a rat preimmune serum.

For actin filament staining, samples were washed 4 times with PBS-0.1% saponin (Research Organic Inc., Cleveland, Ohio), and permeabilized with PBS-0.3% saponin with 50 mM NH_4Cl for 30 min, at RT. Then, they were incubated in a wet chamber with Phalloidin-FITC (1:5 in TBS-T) (Sigma Chemical Co., St. Louis) for 20 min, at RT. Phalloidin-FITC-positive controls were performed on HEp-2 cells.

After washing with PBS-T, nuclei from all samples were counterstained for 2 min with propidium iodide (1:1000) (Vector Laboratories, Burlingame CA), washed and cover-slipped in Vectashield mounting medium (Vector Laboratories, Burlingame, CA). Observations were achieved by a laser-scanning confocal imaging system: FV300 Olympus ATL, with Laser combiner FV5-COMB (Ar Laser, 488 nm; Kr laser, 568 nm). From each cryo-section, 10 fields were imaged. Four to ten serial optical z-sections (0.5 µm thick) were collected from each channel using the dual or triple channel imaging with FITC exciter filter (494 nm) and propidium iodide or TRITC excitation (554 nm). The resulting optical sections were fully projected into two-dimensional planes using the imaging processing system of the microscope (Camos package).

Quantitative analysis

In order to perform a statistical analysis of labelling for vimentin, actin, and tubulin, and to assess the variation of these cytoskeleton components between normal and OA cartilages, pixel intensity of the fluorescent labelling was scored by means of a Confocal Assistant Version 4.02 (MRC/Cas software Bio-Rad).

The study was performed on x40 confocal images from 3 normal (N) and 3 OA cartilages; from each sample (N and OA) 3 slides were made. From each slide 3 or 4 microscopic fields were registered for vimentin, actin and tubulin. This makes a total of 10 of scores for each cytoskeletal component.

The mean ± SEM of the pixel intensity from each sample was determined in order to analyse the variations in fluorescence intensity among the three cytoskeleton components. The statistical analysis was performed by using unpaired t test and the method of Kolmogorov and

Smirnov (Table 1).

To determine the percentage of fluorescence intensity per field, the red staining of nuclei (R) was taken as 100%. The percentage of green labelling (G) for vimentin, actin, and tubulin was calculated by applying a simple equation: G/R X 100 = % (Kouri et al., 2002).

Western blot

To assess possible alterations in the integrity of the cytoskeleton proteins, knee cartilages (a pool from 30 normal rats and a pool from 60 OA rats) were used. Tissues were separated from the bone, with the aid of a stereoscopic microscope, cut into small pieces, pulverized in liquid nitrogen and stored at -70 °C. Each pool from normal and OA powdered cartilage (500 mg wet weight) was homogenized in 5 ml acetate buffer (50 µM sodium acetate, pH 5.8), supplemented with protease inhibitor cocktail (1 mM PMSF, 3 mM IA, 3 mM NEM), 1 mM EDTA, and 4 M guanidine hydrochloride. Extracts were stirred overnight at 4 °C and dialyzed against 200 volumes of Tris/acetate buffer (50 mM Tris-HCl, pH 7.4, 50 mM sodium acetate, pH 7.4, 0.15 M NaCl, 1 mM EDTA) for 4 h (Fryer et al., 1992). To further increase the solubility of the cartilage, 50 µl lysis buffer (4 M urea, 2% Triton X-100) supplemented with 5 µl protease inhibitor cocktail together with 50 µl of sample buffer (50 mM Tris-HCl, pH 6.8, 25% vol/vol glycerol, 2% SDS, 0.02% pironin "Y") containing 5 % of 2ß–mercaptoethanol, were added to 500 µl of each type of sample. Afterwards, the aliquots were homogenized in a vortex and boiled for 3 min. Extracts were centrifuged at 200xg for 1 min at 4 °C, and 10 µl of the supernatant was resolved in a 10% SDS-polyacrylamide gel, according to Laemmli (1970). Protein concentration in each lane was evidenced by the Coomassie blue stain (data not shown). Molecular weight markers ranged from 45 to 200 kDa (Bio-Rad). Blotting to nitrocellulose paper (Bio-Rad) was done according to the Towbin method (Towbin et al., 1979). Gels were transferred at 20 V overnight; filters were washed with TBS-T (100 mM Tris-HCl, 1.5 M NaCl, 0.05% Tween-20, pH 7.4). Blocking was carried out with 5% skimmed milk (Svelty, Nestle) in TBS-T, for 1 h. For the immunoenzymatic assay, nitrocellulose strips were incubated with the appropriate primary antibody (anti-vimentin 1:200, Oncogene Research Products; anti-actin 1:50, Oncogene Research Products; and anti-ß-tubulin 1:50, Santa Cruz, Biotechnology, USA,) for 1 h at RT. After washing with TBS-T, filters were incubated with the secondary antibody conjugated with alkaline phosphatase (1:5000), for 1 h at RT, washed with TBS-T and developed with 33 ml NBT (nitro blue tetrazolium, Sigma), 66 ml BCIP (5-bromo-4-cloro-3-indolyl phosphate, Sigma) in 10 ml AP (100 mM Tris-HCl, 100 mM NaCl, 5 mM MgCl, pH 9.5). The obtained bands were compared with their respective Mr standards run in parallel: vimentin = 57 kDa; actin = 45 kDa; and tubulin = 55 kDa. Vimentin standard was purified from the monkey Vero fibroblast cellular line according to Franke et al. (1981).

Extracts from normal chondrocytes cultured in alginate pearls were prepared without guanidine and urea in order to discard artificial degradation of the cytoskeleton components.

Results

The three cytoskeleton components studied displayed remarkable differences in their distribution pattern, concentration, and percentage of labelled cells when comparing normal and OA-induced cartilage. These differences were within dissimilar regions of the tissue and frequently among neighboring cells.

Ultrastructure

Normal cartilage

The intermediate filament cytoskeleton in chondrocytes showed a uniform distribution as perinuclear cytoplasmic bundles of 10-15 nm in diameter (Fig. 1A).

OA cartilage

The intermediate filament cytoskeleton in OA chondrocytes from the superficial zone showed variable rearrangements, from a simple disorganization to a total cytoplasmic architecture disruption (Fig. 1B).

Immunohistochemistry

Normal cartilage

All chondrocytes displayed a typical labelling pattern for each cytoskeleton component; vimentin appeared abundantly in perinuclear filaments widespread through the cytoplasm toward the periphery of the cells (Fig. 2A,B). The actin labelling was observed mostly as a dense layer just beneath the plasma membrane of the chondrocytes (Fig. 2D,E), whereas tubulin immunolabelling was present throughout the entire cytoplasm displaying a thick mesh-like granular pattern (Fig. 2G,H).

OA cartilage

The cytoskeleton of OA chondrocytes, when compared with chondrocytes from normal tissue, displayed a disordered distribution within cells. For vimentin, some OA chondrocytes displayed a thick granular immunolabelling, which was poorly observed or even absent in neighboing cells (Fig. 2C). Actin labelling was abundantly observed within some chondrocytes, whereas in some neighbouring cells it was remarkably fragmented or absent (Fig. 2F). Tubulin labelling showed a fine granular and fragmented

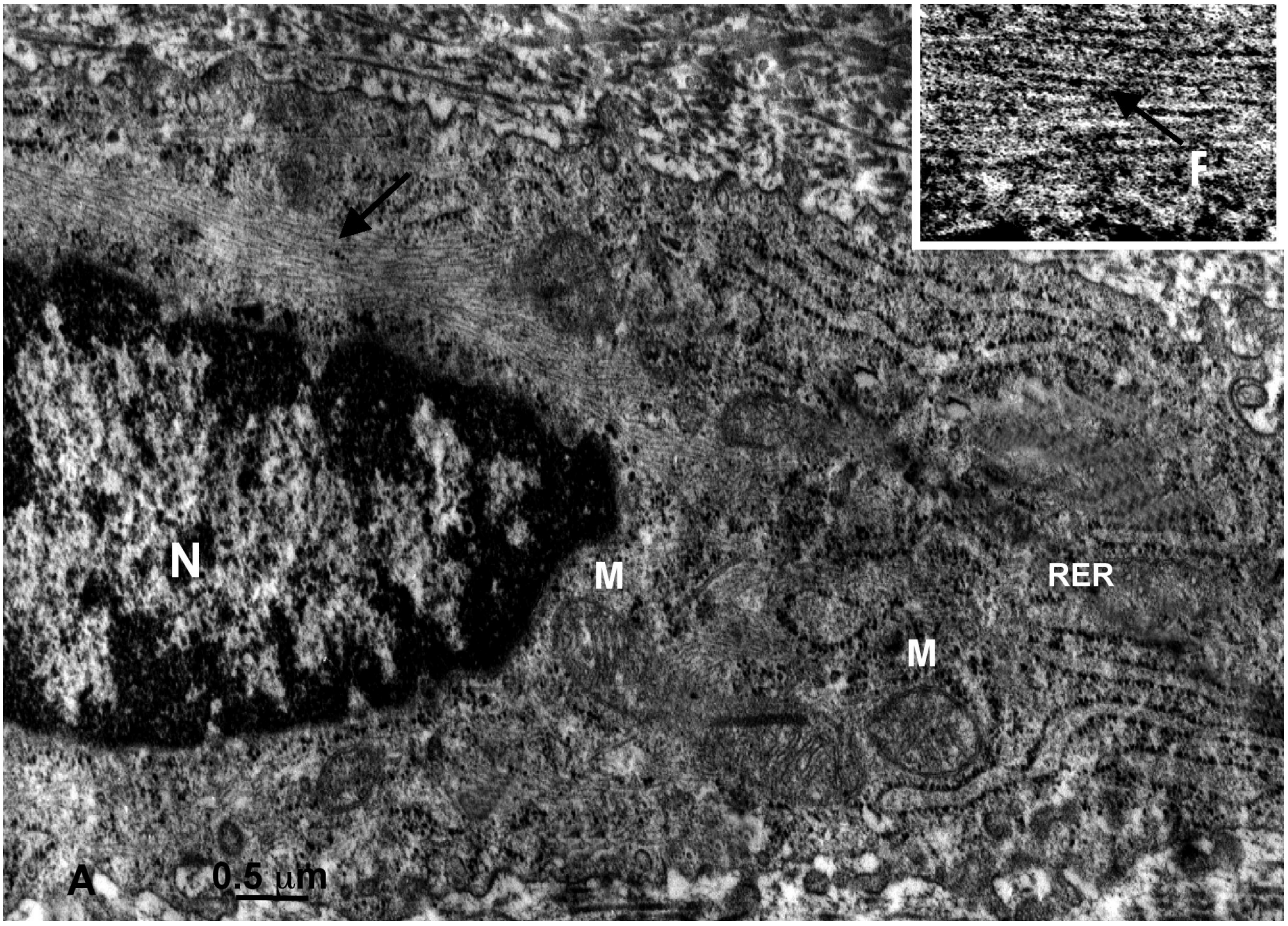

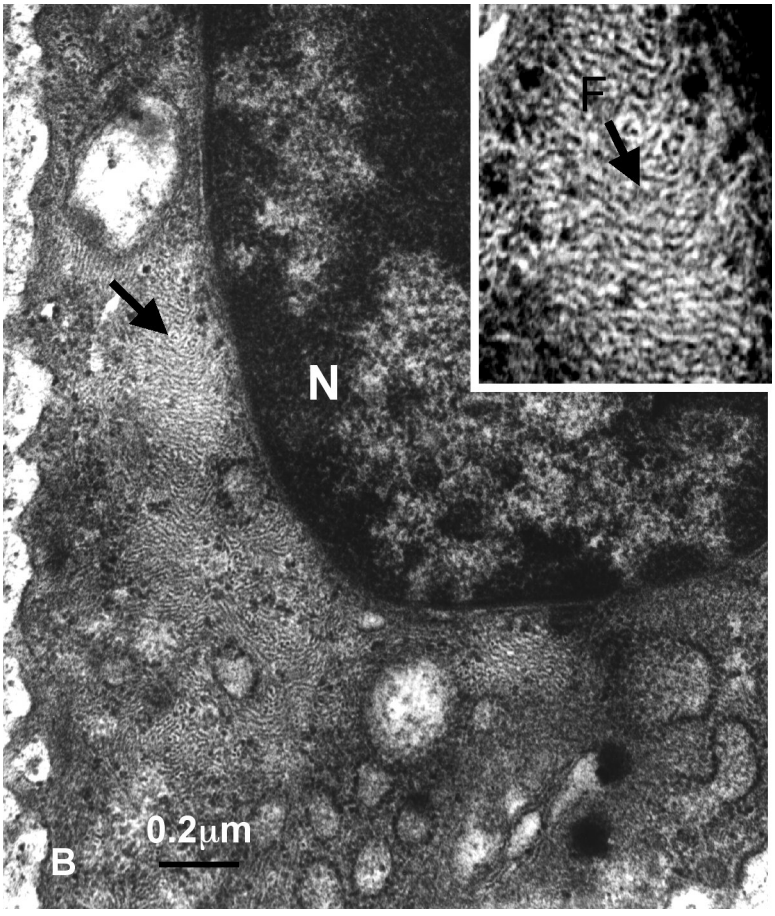

Fig. 1. Electron micrographs. **A.** Normal chondrocyte: chondrocyte displaying bundles of perinuclear intermediate filaments (arrow), nucleus (N), rough endoplasmic reticulum (RER), and mitochondria (M). x 10,000. **Inset:** Higher magnification of the intermediate filaments. Notice the integrity of the filaments (arrow). 33,000. **B.** OA chondrocyte. Notice the disordered and fragmented intermediate filaments (arrow), nucleus (N). x 20,000. **Inset:** Fragments of the filaments are observed (arrow). 52,000

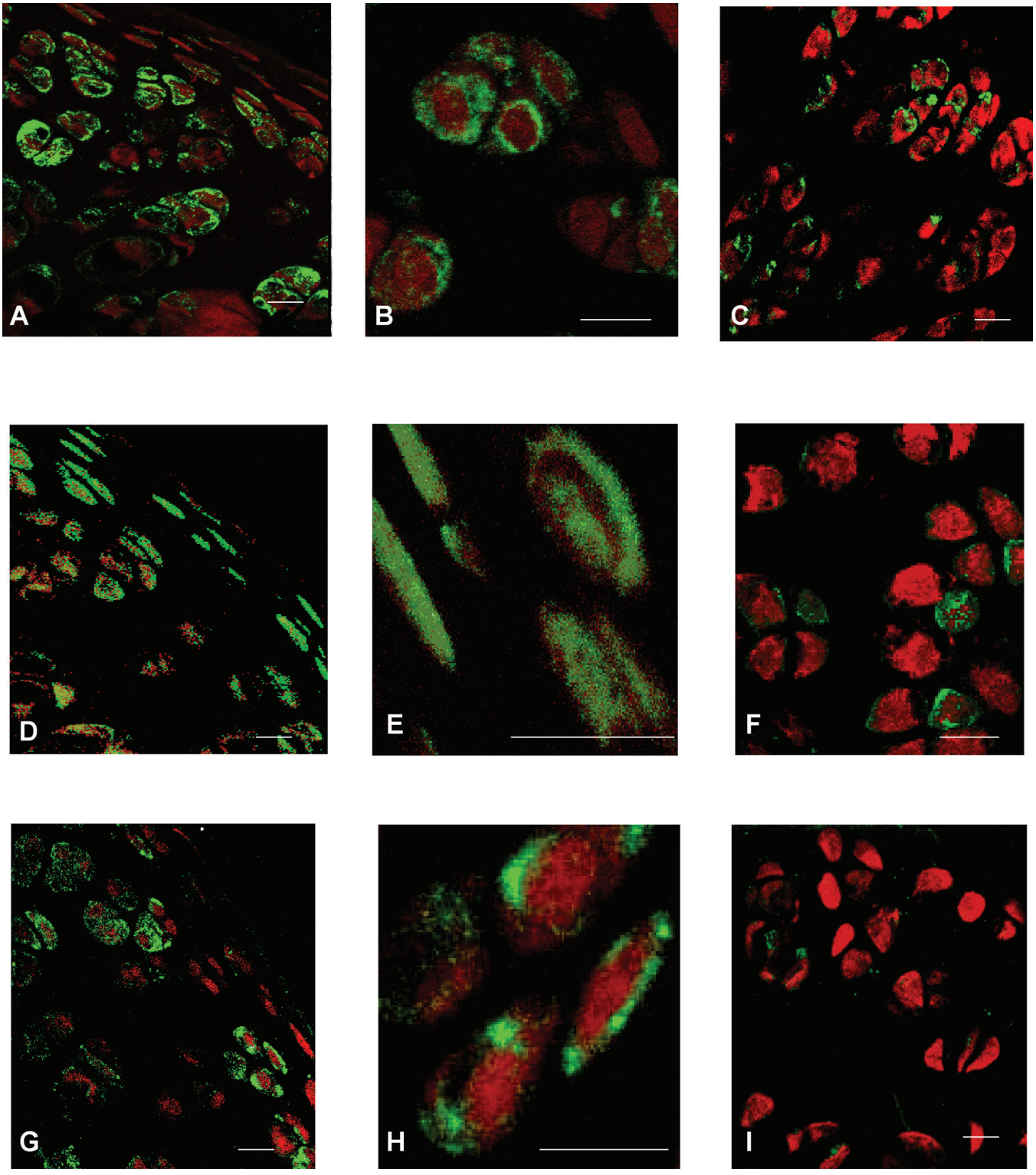

Fig. 2. Fluorescence staining of the distribution from cytoskeleton components. In all cases specific staining is achieved with FITC (green) and nuclei are counterstained with propidium iodide (red). **A-C.** Vimentin immunolabellings. **A, B.** Notice the distribution of labelling within normal chondrocytes, mostly located in the middle and upper-middle zones of the cartilage (arrows). **C.** OA chondrocytes showing scarce and disperse immunolabelling (arrows). **D-F.** Actin labellings. **D, E.** Observe the distribution pattern of actin on the surface of the normal chondrocytes which are mainly located within the entire depth of the cartilage (arrows). **F.** Some OA chondrocytes exhibit immunolabelling, while in neighboring cells immunolabelling is completely absent (arrows). **G-I.** Tubulin immunolabellings. **G, H.** Notice the distribution pattern within normal chondrocytes (arrows), which are mainly located in the middle and upper-middle zones of the cartilage. **I.** OA chondrocytes exhibit scarce and even absent immunolabelling (arrows). Bars: 10 µm.

immunolabelling that varied from cell to cell (Fig. 2I).

Quantitative score of labelling intensity in OA-induced rat cartilage

Labelling patterns showed great variability among neighboring cells in the same field and frequently at different microscopic fields within the same sample. The averages of labelling percentage were determined. Normal cartilages showed a percentage of labelling of 63.94% for vimentin, 55.6% for actin and 37.4% for tubulin. OA cartilages showed a 26.8% for vimentin, 50.1% for actin, and 17.3% for tubulin. Therefore the decrease in percentage of labelling of the OA-induced cartilage in comparison with normal cartilage was 37.1% for vimentin, 4.7% for actin, and 20.1% for tubulin (Table 1).

In addition, statistical analysis between samples from normal and OA cartilage showed a highly significant difference for vimentin, a significant difference for tubulin, and a non-significant difference for actin (Table 1).

Western-blot

In order to confirm that cytoskeleton alterations were associated with OA development, Western blot analysis of cartilage extracts was performed for each one of the three main cytoskeleton proteins.

As observed in Fig. 3A, for vimentin, normal cartilage showed three bands of 57, 55, and 46 kDa. On the contrary, OA cartilage showed a more complex pattern of bands, from 55 kDa to 38 kDa. The 57 and 55 kDa bands were also present in normal cultured chondrocytes that were not treated with guanidine and urea; under this condition, the 46 kDa band was not observed. In the case of actin (Fig. 3B), only a 45 kDa band was detected in all conditions. However, with

Table1. Quantitative scoring of immunolabelling intensities and statistical analysis.

GROUP	RAT	N[a]	RED[b]	GREEN[c]	% REDUCTION[d]	MEAN±SEM	P<0.05
V	N	10	41.6±5.42	26.6±3.6 (63.9%)	37.1	65.70±5.72	***
	OA	10	36.5±3.2	9.8±1.18 (26.8%)		28.58±3.89	<0.0001
A	N	10	13.6±1.37	7.56±1.05 (55.6%)	4.7	58.79±7.13	ns
	OA	10	12.9±1.52	6.56±1.16 (50.1%)		50.92±6.04	0.4117
T	N	10	25.7±2.57	9.60±1.31 (37.4%)	20.1	40.13±5.65	*
	OA	10	21.1±2.1	3.64±0.84 (17.3%)		19.24±5.43	0.0395

[a]: Number of scored microscopic fields. [b]: Intensity of red pixels (nuclei): mean±SEM. [c]: Intensity of green pixels for vimentin, actin, and tubulin: mean ± SEM. [d]: Percentage of immunolabelling reduction (%) between normal (N) and OA rats. Statistical analysis is performed using unpaired t test and the method of Kolmogorov and Smirnov for vimentin (V), actin (A), and tubulin (T) with respect to their mean percentage of labelling for normal (N) and OA rats. Highly significant difference (***). Significant difference (*). Non- significant difference (ns). Standard Error Mean (SEM).

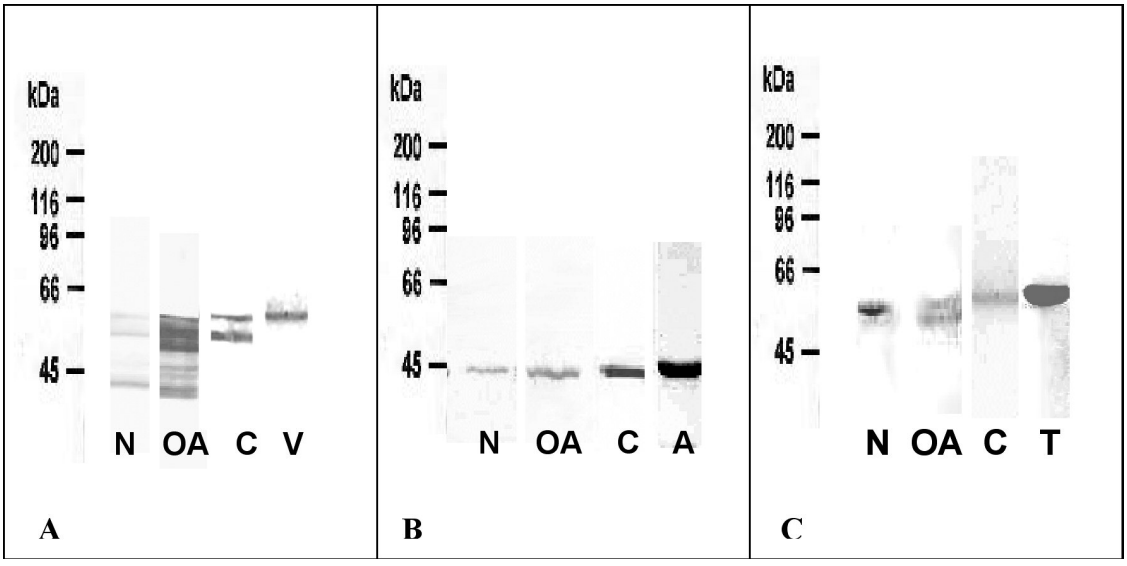

Fig. 3. Western blot of rat cartilage extract pool. With anti–vimentin monoclonal antibody and vimentin standard (V), anti- actin antibody and actin standard (A) and anti- tubulin antibody and tubulin standard (T). There are different reactions in: OA-induced rat cartilage (OA), and normal cartilage rat (N), control normal chondrocytes of culture in alginate pearls (C) without guanidine and urea treatment. Notice the double band (55 and 57 kDa).

tubulin (Fig. 3C) the OA cartilage showed two bands of 55 and 57 kDa whereas normal cartilage as well as cultured chondrocytes showed only one band at 57 kDa.

Discussion

Using three different technical approaches, our results demonstrated that OA-induced rat chondrocytes displayed a remarkable and variable modification of the cytoskeleton architecture. Changes in intermediate filament cytoskeleton from OA cells, were observed when compared to normal chondrocytes. The present findings agree with previous results regarding the intermediate filaments in human OA (Kouri et al., 1998).

The variability and heterogeneity of fluorescence labelling observed among the different cytoskeleton components were evident. Fluorescent staining assays showed that in normal cartilage the percentage of labelling for vimentin and actin was higher than for tubulin. Although labelling intensity in OA cartilage, compared to normal cells, decreased for all cytoskeleton components, we found that actin showed the highest percentage, followed by vimentin, and tubulin, thus indicating that actin may be the least disrupted protein in OA chondrocytes. On the other hand, labelling heterogeneity of the cytoskeleton observed in each microscopic field could be related to different stages of the chondrocyte metabolism and more precisely to their catabolism, specially in OA.

Western blot was a very useful tool to corroborate the ultrastructural and fluorescence findings. By this technique, vimentin showed an altered pattern in OA cartilage with clear differences to normal cartilage supporting the results obtained with transmission electron microscopy where intermediate filaments were the most altered. However, normal chondrocytes displayed a double band at 55 and 57 kDa, and another at 46 kDa, where the last two might be considered as degradation products. An experimental control, accomplished with normal chondrocyte suspension (Häuselmann et al., 1996; Huerta, 2000), in which the solubilization procedure using guanidine and urea treatment was omitted, showed two bands for vimentin (55 and 57 kDa). Actin in OA samples showed one specific band (45 kDa). In the case of the electrophoretic pattern of tubulin in normal cartilage, a sharp and clearly defined band was observed, whereas in OA samples tubulin appeared partially degraded. These results suggest that actin was the less affected protein, while tubulin and vimentin were the most altered.

Interestingly, similar results by western blot assays were obtained in human OA cartilage (unpublished data). Normal human cartilage displayed only one 55 kDa band for vimentin, whereas OA cartilage showed several bands between 55 to 38.5 kDa. Actin showed only one band of 45 kDa in both normal and OA cartilage, and with tubulin a simple band (57 kDa) in the normal cartilage and an extra band of 32 kDa in the OA sample were found.

Changes in the cytoskeleton described here might correlate with different phenomena previously reported in OA cartilage, such as those found in the Golgi apparatus (Kouri et al., 2002), cellular death by apoptosis (Kouri et al., 1997; Blanco et al., 1998; Hashimoto et al., 1998), or changes in catabolic synthesis activity described during extracellular matrix degeneration (Pelletier et al., 1993; Martell-Pelletier et al., 1994; Abbud-Lozoya and Kouri, 2000). The latter process, in which the cells may be "free floating" could explain the different morphology between clustered and non-clustered chondrocytes in the current scenario. Another process such as cell division, which is the phase of the cell-cycle where dramatic changes of the cytoskeleton occur, might correlate with cytoskeleton disruption, involving microtubule disassembly. In a kinetic study of the morphological changes in the rat OA model (Kouri et al., 2002), cartilages from 0 to 60 days after surgical OA induction were analyzed and no mitosis figures were found.

It would be of great interest to establish whether the cytoskeleton modifications described here lead to OA disease or if OA development is a consequence of cytoskeleton changes. Our results, obtained in a model of OA induced in rat, bring a new focus on the possible cell alterations implicated in the disease pathogenesis. Similar results have been observed in human OA chondrocytes; therefore, the present study might plausibly be a window of comparison to human OA pathogenesis.

The dissection of the cellular mechanisms of this articular degenerative disease may shed more light on its pathogenesis, an important feature for the search for new therapeutic strategies.

Acknowledgements. We are grateful to Dr. Raúl Mena and Biol. José Luna from the Physiology Department, Biophysics and Neurosciences, CINVESTAV-IPN, Mexico City, Mexico for the laboratory facilities, to QFB Ma. Elena Montero for the Western blot assessment, to QFB Sirenia Gonzales and Biol. Lourdes Rojas for the Electron Microscopy Unit (CINVESTAV-IPN) and to Biol. Magdalena Miranda and Biol. Leticia Pérez for their technical assistance and to Clara Castelán for secretarial support. This study was supported by CONACYT grant #28100M and by the Experimental Pathology Department of CINVESTAV-IPN.

References

Abbud-Lozoya K. and Kouri-Flores J.B. (2000). A novel rat osteoarthrosis model to assess apoptosis and matrix degradation. Pathol. Res. Pract. 48, 1307-1320.

Bajo M., Yoo B.C., Cairns N., Gratzer M. and Lubec G. (2001). Neurofilament proteins NF-L, NF-M and NF-H in brain of patients with Down syndrome and Alzheimer's disease. Amino Acids 21, 293-301.

Benjamin M., Archer C.W. and Ralphs J.R. (1994). Cytoskeleton of cartilage cells. Microsc. Res. Tech. 28, 372-377.

Blanco F.J., Guitian R., Vázquez-Martul E., de Toro F.J. and Galdo F.

(1998). Osteoarthritis chondrocytes die by apoptosis. A possible pathway for osteoarthritis pathology. Arthritis Rheum. 41, 284-289.

Egerbacher M., Seiberl G., Wolfesberger B. and Walter I. (2000). Ciprofloxacin causes cytoskeletal changes and detachment of human and rat chondrocytes in vitro. Arch. Toxicol. 73, 557-563.

Franke W.W., Schiller D.L., Moll R., Winter S., Schmid E., Engelbrecht I., Denk H., Kreplrv R. and Platzer B. (1981). Diversity of cytokeratins. J. Mol. Biol. 153, 933-952.

Fryer H.J.L., Kelly G.M., Molinaro L. and Hockfield S. (1992). The high molecular weight Cat-301 chondroitin sulfate proteoglycan from brain Is related to the large aggregation proteoglycan from cartilage, aggrecan. J. Biol. Chem. 267, 9874-9883.

Hashimoto S., Ochs R.L., Komiya S. and Lotz M. (1998). Linkage of chondrocyte apoptosis and cartilage degradation in human osteoarthritis. Arthritis Rheum. 41, 1632-1638.

Häuselmann H.J., Masuda K., Hunziker E.B., Neidhart M., Mok S.S., Michel A.B. and Thonar E.J. (1996). Adult human chondrocytes cultured in alginate form a matrix similar to native human articular cartilage. Am. J. Physiol. 271, 742-752.

Hirsch M.S. and Hartford Svoboda K.K. (1993). Confocal microscopy of whole mount embryonic cartilage: Intracellular localization of F-actin, chick propyl-hydroxylase and type II collagen m-RNA. Micron 24, 587-594.

Huerta Pérez G.M. (2000). Aislamiento y mantenimiento tridimensional de condrocitos de rata Wistar adulta como modelo en el estudio de la osteoartrosis experimental. Tesis de Licenciatura. Facultad de Estudios Superiores Cuatitlán, UNAM. Cuatitlán, Izcalli, Edo. de México, México.

Idowu B.D., Knight M.M., Bader D.L. and Lee D.A. (2000). Confocal analysis of cytoskeletal organization within isolated chondrocyte sub-populations cultured in agarose. Histochem. J. 32, 165-174.

Kouri J.B., Jimenez S.A., Quintero M. and Chico A. (1996). Ultrastructural study of chondrocytes from fibrillated and non-fibrillated human osteoarthritic cartilage. Osteoarthr. Cartilage 4, 111-125.

Kouri J.B., Rosales-Encina J.L, Chaudhuri P.P., Luna J. and Mena R. (1997). Apoptosis in human osteoarthritic cartilage: a microscopy report. Med. Sci. Res. 25, 245-248.

Kouri J.B., Argüello C., Luna J. and Mena R. (1998). Use of microscopical techniques in the study of human chondrocytes from osteoarthritic cartilage: An overview. Microsc. Res.Tech. 40, 22- 36.

Kouri J.B., Aguilera J.M., Reyes J., Lozoya K.A. and Gonzalez S. (2000). Apoptotic chondrocytes from osteoarthrotic human articular cartilage and abnormal calcification of subchondral bone. J. Rheumatol. 27, 1005-1019.

Kouri J.B., Rojas L., Pérez E. and Abbud-Lozoya K. (2002). Modifications of Golgi Complex in Chondrocytes from Osteoarthrotic (OA) Rat Cartilage. J. Histochem. Citochem. 50, 1333-1339.

Laemmli U.K. (1970). Cleavage of structural proteins during assembly of the head of bacteriophage T4. Nature 227, 680-685.

Langelier E., Suetterlin R., Hoemann C.D., Aebi U. and Buschmann M.D. (2000). The chondrocyte cytoskeleton in mature articular cartilage: structure and distribution of actin, tubulin and vimentin filaments. J. Histochem. Cytochem. 48,1307-1320.

Mankin J.H., Mow V.C., Buckwalter J.A., Lannotti J.Q. and Ratcliffe A. (1994). Form and function of articular cartilage. In: Orthopaedic basic science. Simons S.R. (ed). Rosemont I. L.: American Academy of Orthopedic Surgeons. pp 1-44.

Mashima T., Naito M. and Tsuruo T. (1999). Caspase-mediated cleavage of cytoskeletal actin plays a positive role in the process of morphological apoptosis. Oncogene 18, 2423-2430.

Mow V.C., Ratcliffe A. and Poole A.R., (1992): Cartilage and diarthrodial joints as paradigms for hierarchical materials and structures. Biomaterials 13, 67-97.

Martel-Pelletier J., MacCollum R., Fujimoto N., Obata K., Cloutier J.M. and Pelletier J.P. (1994). Excess of metalloproteases over tissue inhibitor of metalloproteases may contribute to cartilage degradation in osteoarthritis and rheumatoid arthritis. Lab. Invest. 70, 807-815.

Pelletier J.P., Faure M.P., Di Batista J.A., Roughley P., Wilhelm S., Visco D. and Martel-Pelletier J. (1993). Coordinate synthesis of stromelysin, interleukin-1 and oncogene protein in experimental osteoarthritis: An immunohistochemical study. Am. J. Pathol. 142, 95-105.

Pena S.D., Opas M., Turksen K., Kalnins V.I. and Carpenter S. (1983). Immunocytochemical studies of intermediate filament aggregates and their relationship to microtubules in cultured skin fibroblasts from patients with giant axonal neuropathy. Eur. J. Cell Biol. 31, 227-234.

Sigal M.J., Aubin J.E. and Ten Cate A.R. (1985). An immunocytochemical study of the human odontoblast process using antibodies against tubulin, actin, and vimentin. J. Dent. Res. 64, 1348-1355.

Takeda M., Tatebayashi Y. and Nishimura T. (1992). Changes in the cytoskeletal system in fibroblast form patients with familial Alzheimer's disease. Prog. Neuropsychopharmacol. Biol. Psychiatry 16, 317-328.

Towbin H., Staehelin T. and Gordon J. (1979). Electrophoretic transfer of proteins from polyacrylamide gels to nitrocellulose sheets: procedure and some applications. Proc. Natl. Acad. Sci. USA 76, 4350- 4354.

Zanetti N.C. and Solursh M. (1984). Induction of chondrogenesis in limb mesenchymal cultures by disruption of the actin cytoskeleton. J. Cell Biol. 115-123.

Accepted May 7, 2004